

Robotic origami folding

Devin J. Balkcom
Department of Computer Science
Dartmouth College
Hanover, NH 03755
devin@cs.dartmouth.edu

Matthew T. Mason
Robotics Institute
Carnegie Mellon University
Pittsburgh, PA 15213
matt.mason@cs.cmu.edu

Abstract

Origami, the art of paper sculpture, is a fresh challenge for the field of robotic manipulation, and provides a concrete example for many difficult and general manipulation problems. This paper describes our initial exploration, and highlights key problems in manipulation, modeling, and design of foldable structures. Results include the first origami-folding robot, a complete fold-sequence planner for a simple class of origami, and analysis of the kinematics of more complicated folds, including the common paper shopping bag.

1 Introduction

Humans are far more skilled than robots at manipulating flexible, unpredictable materials. The clearest example is origami, the human art of paper sculpture. Figure 1 shows the state of the art in robotic origami folding – a simplified samurai hat being folded by a robot in our lab. Figure 2 shows *Icarus*, folded by master Hojyo Takashi out of a single piece of paper, without cutting or gluing.

This paper examines origami from the perspective of robotic manipulation. There are many compelling reasons to explore and better understand folding manipulation, and origami provides a useful starting point.

A better understanding of techniques for designing and folding flexible structures would be of great practical use. In the past, automated manufacturing with rigid bodies was the driving application for the study of robotic manipulation; tasks include grasping, fixturing, pushing, sorting, and feeding. Applications of deformable manipu-

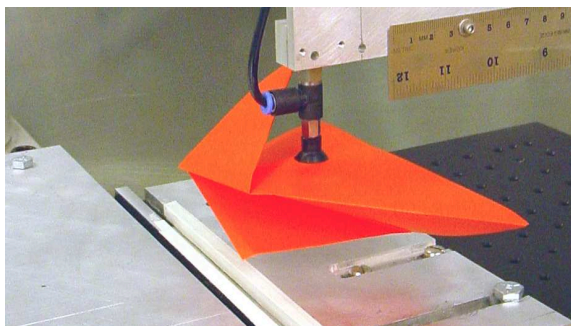


Figure 1: A simplified samurai hat being folded by a robot.

lation include paper bags, garments, fast-food containers, sheet-metal, car airbags, space-telescope mirrors, and MEMS. Building products out of thin sheets may reduce material costs, and allow storage in small volumes.

Origami also reveals limitations of the state-of-the-art in robotic manipulation. Hardware is one problem. Humans have dozens of degrees of freedom in their hands, touch-sensitive skin, and capable binocular vision. The industrial robot that forms the core of our paper-folding machine has four degrees of freedom, and does not sense the paper – the robot could be compared to a blind man with no sense of touch folding origami with one finger.

The primary challenges, however, are algorithmic. We do not know how to manipulate, model, or design foldable structures.

The first challenge is minimalist manipulation. Paper has infinite degrees of freedom, and sensing and control are hard. Occlusion, the thin-ness of the paper, and the presence of curved surfaces are challenges for vision



Figure 2: An example of the state-of-the-art in human folding: *Icarus*, by Hojyo Takashi; dry-folded out of a single piece of paper. Photograph used by permission.

or laser-range-finding. Tactile sensors are even worse – touching the paper is likely to deform it.

Humans have some tricks for manipulating paper in spite of the sensing difficulty. Figure 3 shows an example. The goal is to fold a precise diagonal crease. The folder grasps two corners and brings them into precise alignment. The fingers of one hand then flatten the bulge in the paper. Since the paper does not stretch, a crease forms at the extreme region of the paper, along the diagonal. The fingers extend and sharpen the crease. The process requires minimal sensing, with only a few degrees of control. We would like to build robots that use similar techniques, but our first attempt is much more crude: the robot places creases using a vice-like clamp that flattens the paper near the crease.

The second challenge is modeling. Even if we model folding paper as a collecting of rigid facets connected by hinges at the creases, the configuration space of a foldable structure may be complicated. The simplest model of creased paper is a collection of rigid bodies with hinges. If creases meet at a vertex, the mechanism is a kinematic

closed chain.

Traditional sampling-based path planners struggle with environments containing narrow corridors. The configuration space of a closed chain may be a union of several manifolds, containing infinitely thin corridors. The probability that a random-sampling planner will find a path between two points on different manifolds is zero, if every path must contain points on a connecting region of lower dimension.

In this paper, we present a few configuration-space parameterizations that allow local planning, and discuss geometric techniques for analyzing the global topological structure of the configuration space.

The third challenge is design. Not all patterns of creases fold equally well. For example, we show that the common paper shopping bag cannot be folded without flexing or bending the paper in regions where there are no creases. How complicated a model is necessary to describe the folding of a shopping bag, and can creases be added so that the bag folds predictably? Ultimately, we want to design software that can automatically create crease patterns that allow one shape to be folded into another smoothly, while maximizing rigidity at the initial and final configurations.

1.1 The task domain

There are many levels of origami complexity. The simplest traditional origami designs require only sequential straight-line folds. At the next level of complexity, birds, frogs, and the waterbomb require multiple creases that meet at a vertex to be manipulated simultaneously, while modern three-dimensional insects and flowers require multi-vertex networks of creases to be manipulated simultaneously. State-of-the-art origami sculpture requires even more complicated techniques. Masks require bending facets and folding curved creases, animal sculptures are often folded using wet paper, and modular origami requires assembly of several pre-creased sections.

Figure 4 shows our current state of progress. The simplest skills can be implemented on a robot; we have built a robot and automatic planning software to fold simple origami, including paper airplanes, an origami cup, and a simplified samurai hat.

We understand more advanced skills less well. For example, the (unsimplified) samurai hat requires that two

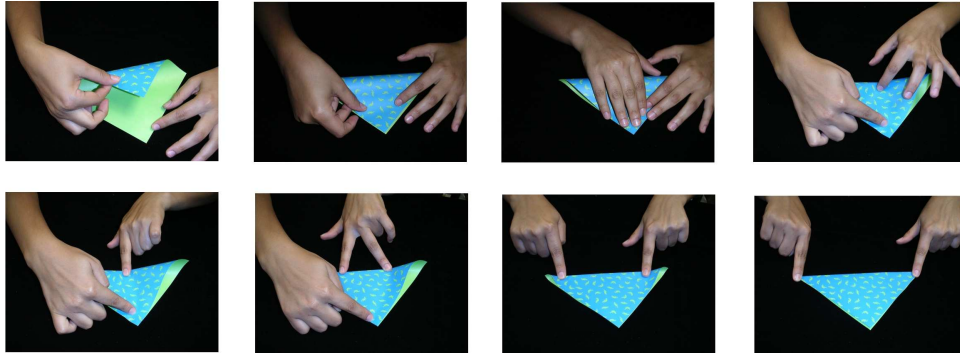


Figure 3: Creating a valley fold using landmarking.

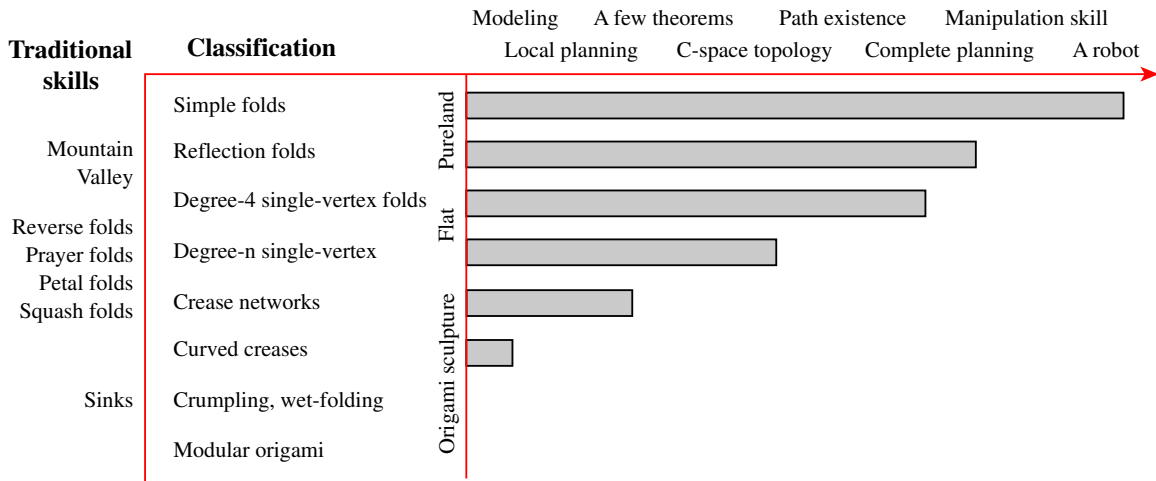


Figure 4: A map of the origami task domain.

coplanar sections of paper be separated so that a flap can be folded. We have built a planner to explore the possible fold-sequences for the samurai hat, but the robot cannot reliably separate facets of paper. The paper crane is yet more complicated; the paper must be precreased and unfolded to create a pattern where multiple creases meet at a vertex. These creases must be manipulated simultaneously, as shown in figure 11. The mechanism is a kinematic closed chain, and motion planning for closed chains is a well-known open problem in robotic manipulation. We can describe local parameterizations of the configuration space that allow local planning, and have techniques for analyzing the global structure of the con-

figuration space, but do not have a complete planner.

We know very little about the most sophisticated origami. We can build mathematical models of origami with curved creases, networks of creases, or curved sections of the paper, but have only studied the simplest of examples.

The structure of the paper follows the map described in figure 4 vertically, from simple folds through crease networks.

1.2 Related work

Box folding and sheet metal bending are the two robotics applications closest to origami folding; see Lu and Akella [Lu and Akella, 1999, Lu and Akella, 2000], Liu and Dai [Liu and Dai, 2003], and Gupta *et al.* [Gupta *et al.*, 1998]. In preliminary work [Balkcom, 2004, Balkcom and Mason, 2004], we focus on the simplest possible model of origami: rigid bodies connected by hinges at the creases. Miyazaki *et al.*'s [Miyazaki *et al.*, 1992] software simulates simple origami manipulation under this model, and a rigid-body model for cartons with origami-like folds has also been studied by Dai, Rees Jones, and Liu [Dai and Jones, 2002b, Dai and Jones, 2005, Dai and Jones, 2002a, Dai and Jones, 1999].

When creases intersect, even the simplest model poses challenges, since the mechanism is a closed chain. Motion of closed chain mechanisms can be simulated efficiently (see Ascher and Lin [Ascher and Lin, 1999]), and the configuration-space topology of spherical closed chains of the type found in origami has been analyzed by Kapovich and Millson [Kapovich and Millson, 1995]; our approach is based on work on planar closed chains by Milgram and Trinkle [Milgram and Trinkle, ming].

In fact, the kinematics of origami mechanisms may provide inspiration for new mechanism designs, as suggested by Rodrigues-Leal and Dai [Rodrigues-Leal and Dai, 2007].

One of the interesting properties of paper is that it bends but does not stretch; such surfaces are said to be *developable*; Hilbert and Cohn-Vossen [Hilbert and Cohn-vossen, 1952] is a good reference. Several authors have used developable surfaces to approximate the state of paper and cloth, including Redont [Redont, 1989], Sun and Fiume [Sun and Fiume, 1996], Leopoldseder and Pottmann [Leopoldseder and Pottmann, 1998], Pottmann and Wallner [Pottmann and Wallner, 1999], Weiss and Furtner [Weiss and Furtner, 1988], and Aumann [Aumann, 1991]. Huffman [Huffman, 1976] considers creases as limiting cases of developables, particularly networks of creases and curved creases. Sometimes creases occur because there are constraints applied that are inconsistent with the paper remaining a smooth developable surface; see Kergosien *et*

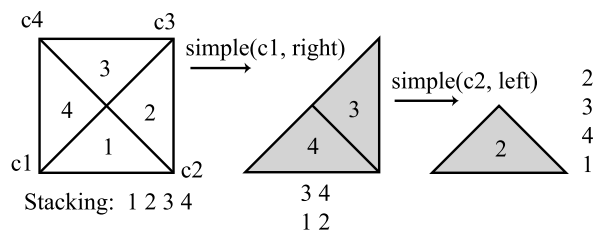


Figure 5: A sequence of two simple folds.

al [Kergosien *et al.*, 1994]. Dynamic simulation of cloth and paper is an active research area in the graphics community. Baraff and Witkin's [Baraff and Witkin, 1998] work is seminal; Choi and Ko [Choi and Ko, 2002] and Bridson *et al* [Bridson *et al.*, 2002] present recent approaches.

There is a rich field of work on origami design in the mathematics community; Demaine *et al.* [Demaine and Demaine, 2001] provides a survey. Robert Lang's papers and TreeMaker software [Lang, 2001] and Hull [Hull, 1994] are usually credited with being the first in-depth work.

1.3 Piecewise-rigid origami

Although the mechanics of folding require that paper bend, it is useful to consider a very simple model of origami composed of rigid polygonal facets connected by revolute joints at the creases. Define the *origami pattern* to be the placement of the creases on unfolded origami. Creases meet at interior vertices of the pattern; if n creases meet, we say that a vertex is of *degree* n . The angles between creases around a vertex in the pattern are called *sector angles*.

Each crease connects two facets. We associate with each pattern a *facet graph*, whose nodes are facets and edges are creases. Any tree that spans the facet graph is a *facet tree*. Facet trees are easy to construct; any complete search method such as breadth-first or depth-first search is suitable.

A facet tree implies a parent-child relationship between two facets connected by a crease. We will choose the convention that all facets are described by a counter-clockwise set of points in the pattern; we will associate a unit vector with each crease such that the vector's direc-

tion agrees with the order of vertices in the child facet. We then describe the *crease angle* as the angle between a parent facet and its child; the sign is chosen to be consistent with the right-hand rule applied to the crease vector.

Given a pattern and any facet tree, the crease angles associated with all uncut creases determine the configuration of the origami mechanism – the pose of each facet and the angle of each cut crease can be determined by traversing the facet tree applying rotations to descendent facets.

Since origami can be folded essentially flat, it is convenient to allow crease angles in the range $[-\pi, \pi]$. The order in which facets are folded becomes important when crease angles reach extreme values and facets become coplanar. We will call a group of coplanar facets a *compound facet*. With each compound facet we associate a normal vector and a partial ordering of facets that describes the order in which the compound facet may be assembled or disassembled: the facet *stacking*. The height of a facet is its height in the stacking, and the height of a crease is the height of its child facet.

2 Simple folds: an origami-folding machine

The most basic origami fold takes all paper on one side of a crease line and folds it to the other side. Figure 5 shows a sequence of two simple folds, described using the rigid origami model, and figure 3 shows a human executing a simple fold. Figure 6(a) shows a machine designed to allow a 4 DOF SCARA robot arm to make simple folds.

The folding procedure is outlined in figure 6(b). The arm grasps the paper using a vacuum pad, and positions the paper over the folding mechanism. A blade presses the paper into a slot in the folding mechanism (step 2); friction holds the paper in the slot as the blade is removed. The slot clamps shut, forming the crease (step 3). Steps 4 and 5 show a method for removing the paper from the slot and placing it flat on the table; this is required since the arm only provides one rotational degree of freedom at the wrist. First the blade sweeps across the paper, forcing it to lie flat. The clamp is released while the blade holds the paper against the table; the springiness of the paper allows it to swing free of the slot.

What can be folded using a sequence of simple folds? Figure 7 shows two examples: a simple paper cup, and a simple paper airplane.

The design of the machine is based on the observation that it is not necessary to flip the paper over at any step, if the sequence of folds is planned carefully:

Fact 1 *Any origami piece that can be folded by a sequence of flips and simple folds can be folded by a single initial flip and a sequence of valley simple folds.*

Proof: A mountain simple fold is equivalent to a flip, valley simple fold, flip sequence; write $m = fvf$. Second, ff is the identity. Third, either the facets on the left or on the right of the crease line can be chosen as the base. Using similar notation, $v_l f = v_r$, and $v_r f = v_l$. These substitution rules imply that any fold sequence can be rewritten to include only a single initial flip and a sequence of valley simple folds. First, remove all mountain folds from the sequence. Then remove all ff . Then each flip except the first is preceded by a valley fold. Remove the flips by changing the direction of each of these valley folds. ■

The most obvious limitation of the machine is that simple folds cannot be used to separate two co-planar flaps of paper. In some cases, careful pre-planning can help with this problem, too. A human being would probably fold the body of the airplane shown in figure 7 first, and separate and fold the wings down as the last step. However, by folding the wings first, as shown in steps 4 and 5, this separation step can be avoided. Section 3 will discuss an automatic fold-sequence planner for simple origami.

3 Reflection folds and fold-sequence planning

The foldings of the hat and paper airplane were planned automatically by a complete sequence planner for simple origami. The input to the planner is the origami pattern and the desired final stacking of the facets in the folded state. The output is a sequence of folds to make, and a set of configurations where the robot arm must place the paper for each fold.

The algorithm is a simple breadth-first search – the flat pattern is the root node of the search tree, and children

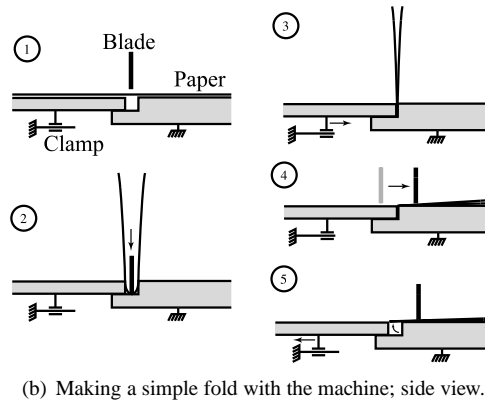
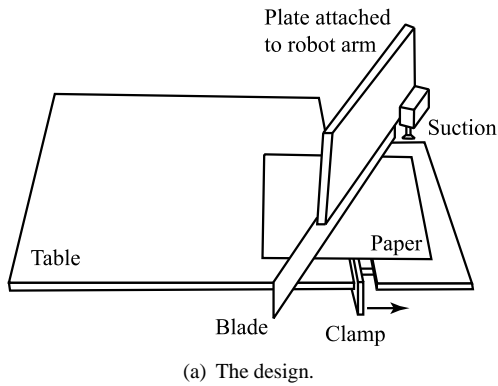


Figure 6: A machine that can fold simple origami.

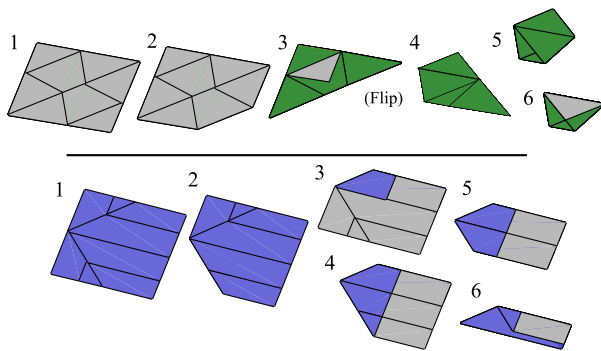


Figure 7: Simple foldings of two traditional origami designs.

of each node are generated by enumerating all possible simple folds.

Given a flat origami state, what simple folds are possible? First, find the minimal set of lines that contains all creases. Discard any crease lines that cross a facet. Each remaining crease line divides the facets into two compound facets; we arbitrarily assign one to be the ‘base’ and one the ‘flap’. During folding, the base will not move. The flap can be folded either up (a *valley simple fold*) or down (a *mountain simple fold*).

To execute the fold, all creases colinear with the crease line are folded simultaneously. During folding, the heights of facets in the flap are reversed, and then either stacked above or below the base, forming a single new compound facet.

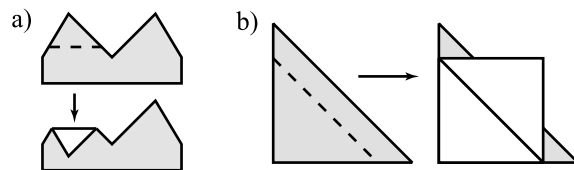


Figure 9: Two designs that can be reflection-folded but not simply-folded.

The algorithm is unfortunately exponential in the number of creases in the pattern. Some efficiency can be gained by storing intermediate configurations and pruning branches of the tree that reach previously-explored configurations; this is described in more detail in section 3.2.

3.1 Reflection folds

Figure 9 shows two examples of origami that cannot be simply folded. We define a *reflection fold*: any fold for which all the active creases are colinear such that the continuous rigid-body rotation of the moving facets does not cause self-intersection of the origami or tear any creases. We will call the moving facets the flap, and the fixed facets the base. All facets lie in a plane both before and after the fold.

The simple folds from an origami state are easy to enumerate. Finding the possible reflection folds is somewhat more complicated. The following observation is useful to limit the number of possibilities that must be considered.

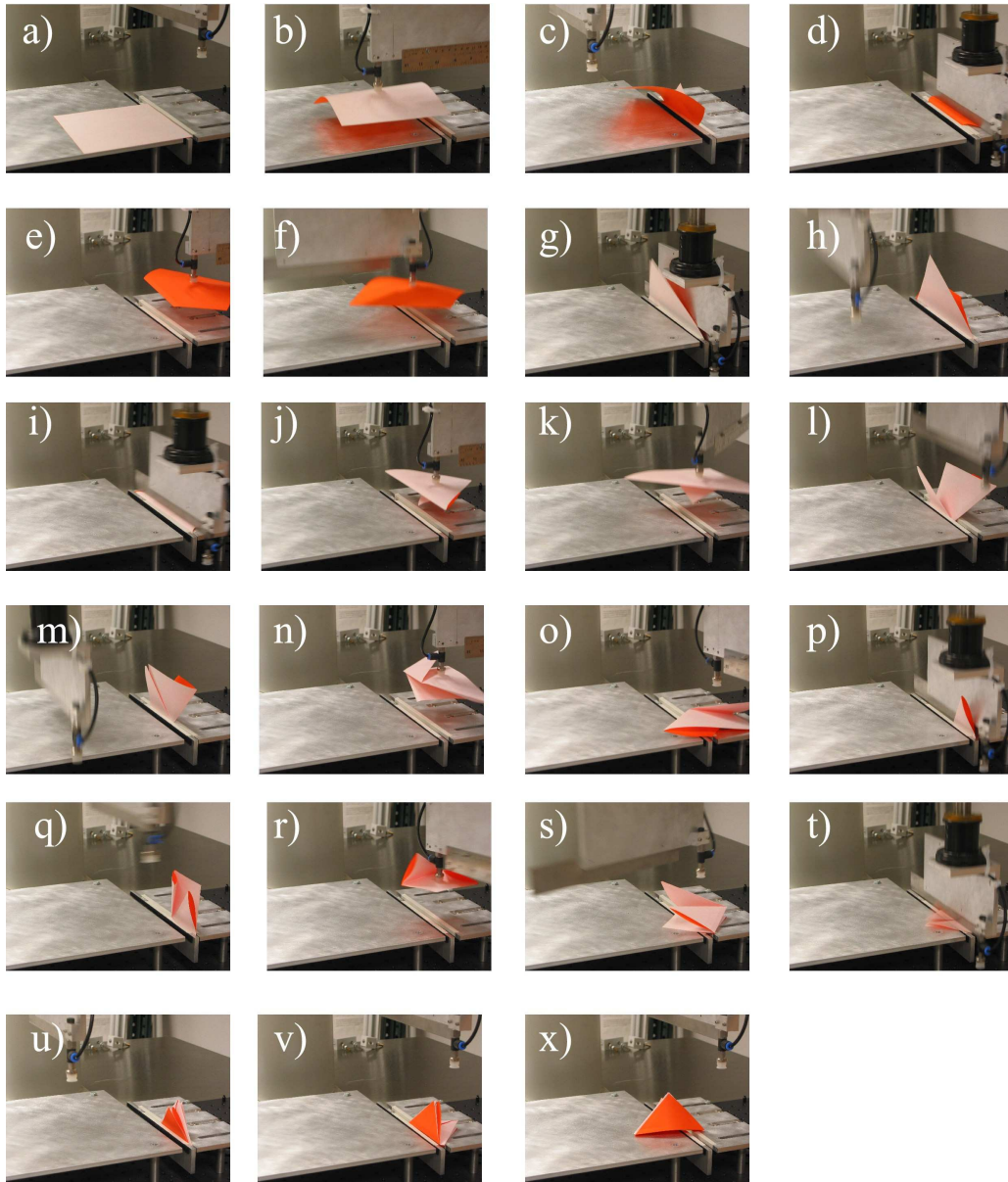


Figure 8: Robotic folding of a paper hat. Subfigures a) through d) show the first crease, e) through i) the second, j) through m) the third, n) through q) the fourth, r) through u) the fifth, and v) and x) show the final product – a folded hat.

Fact 2 *The set of active creases in any fold cuts the facet graph, separating each pair of relatively moving compound facets.*

Proof: Choose two compound facets that move relative to one another; call one the base, and one the flap. Any crease that connects the base and flap and is colinear with the crease line must be active; the crease angle will be the angle between the base and flap, up to sign. Any crease that connects the base and flap but is not colinear with the crease line will be torn by any rotation of the flap around the crease line. ■

We can determine the set of all reflection folds from an origami state, using the following algorithm. First, enumerate all crease lines. Sort the creases by height in the stacking. Consider all sequential combinations of creases that contain either the minimum- or maximum-height crease. Test each of these crease sets to determine if it cuts the facet graph into at least two pieces. All pieces strictly to the left of the current crease line that do not include the root node of the facet tree (which is always fixed) are candidate flaps, as are all pieces strictly to the right. (For simplicity, we do not consider combinations of pieces of the graph as candidate flaps, since combinations can be folded by a sequence of reflection folds.) Test each candidate flap to see if and in which direction(s) folding is possible without self-intersection of the origami; this can be accomplished by polygon intersections in the plane of the compound facet.

The state of the origami after a reflection fold is easy to determine: reflect the flap across the crease line, flip flap stacking, and stack the flap either above or below the base, depending on the direction of the fold.

3.2 Reflection-fold sequence planning

Origami that can be folded using reflection folds is flat after each fold. Since the motion of the flap occurs out of the plane of the base, collision detection is only necessary at the beginnings and ends of folds, and only requires simple polygon intersection tests. Furthermore, the origami state after each fold is just the stacking of the facets, together with the set of creases that have been folded, and is thus discrete. (Note that crease angles can be determined from the stacking, as long as we know which creases have been folded.) We have implemented a complete graph search

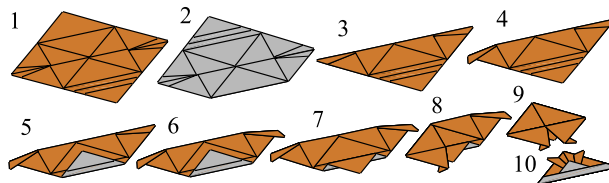


Figure 10: Automatically-planned folding of the samurai hat. With the exception of the reflection fold in step 7, all folds are ‘simple’.

planner for reflection-foldable origami; the nodes of the graph are flat origami states. Figure 10 shows an automatically planned folding of the samurai hat comprised of eight simple folds and one reflection fold.

The input to the planner is the pattern and the desired stacking of the facets. The algorithm is as follows. Use the goal stacking and the pattern to determine signs on the crease angles. Insert the pattern into the search queue as the initial state. While the search queue has elements, pop, test for goal state, and if goal, backchain to find the plan. Otherwise, determine the reflection folds from the state and generate successor states. Cull any states that have crease angles that do not agree with those of the goal state. Also cull any states that have been previously visited. Insert remaining states into the visited list and into the search queue.

The visited list is implemented as a hash table that hashes on the integer heights of facets in the stacking. Before testing against the visited list, the compound facet of the state is collapsed to determine a *minimal stacking*. The algorithm to find the minimal stacking is essentially a bubble sort – each facet is allowed to bubble downwards in the stacking as long as it does not intersect with any facets in the level underneath it.

The planner implementation is about 5000 lines of C++ code, and was run on a 500 mhz Pentium III. The table below shows results for four traditional origami designs.

Origami	creases	nodes	CPU time (sec)	folds
Cup	9	30	.1	5
Airplane	9	24	.1	5
Hat	14	75	.5	5
Samurai hat	20	4250	110	9

For the samurai hat, more than 99% of the CPU time

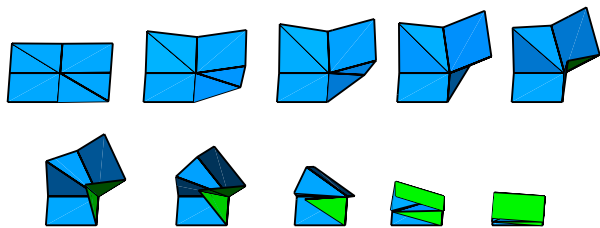


Figure 11: Frames from an animation of the initial ‘prayer fold’ of a crane.

was spent in polygon intersections to determine minimal stackings and to find reflection folds.

4 Kinematics of rigid origami

Many origami designs cannot be reflection folded; figure 11 shows an example. Inside and outside reverse folds, squash folds, and petal folds all manipulate four creases simultaneously.

Analysis of foldability requires that we consider both the kinematics of degree- n folds and the possibility of self-intersection. It is well-known that piecewise-rigid origami with a single vertex has the kinematics of a spherical linkage. The kinematics of degree-four spherical linkages are understood, and we draw on some of these results to further show that self-intersection can only occur when the origami is folded completely flat.

For higher-degree vertices, and origami patterns containing several vertices connected by a network of creases, the problem is more challenging. We present a parameterization of the configuration space for these more complicated mechanisms, but the parameterization describes only the local motion of the mechanism, and not the global structure of the configuration space. In section 5 we present a graphical method for determining this global structure, and analytical results based on Milgram and Trinkle’s work on the topology of the configuration spaces of planar n -bar linkages.

4.1 Self-intersection around degree-four vertices

If one of the crease angles is known, then there are up to two possible configurations of the paper, one ‘elbow-

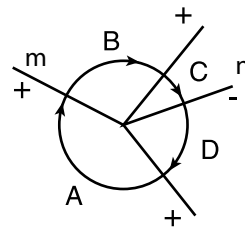


Figure 12: Huffman’s notation for a degree-four vertex.

up’ and one ‘elbow-down’. Huffman [Huffman, 1976] derives a relationship between opposite crease angles m and n for degree-four origami,

$$1 - \cos n = \frac{\sin A \sin B}{\sin C \sin D} (1 - \cos m), \quad (1)$$

where A , D , C , and B are sector angles as shown in figure 12.

The sequence planner for reflection folding described above relies on a key observation – self-intersection can occur only when the origami is flat. We can use Huffman’s formula to show that a similar result holds for origami where four creases that intersect at a vertex are manipulated simultaneously.

To show this, we need a simple lemma:

Lemma 1 *Continuous motions of degree-four origami mechanism cannot cause self-intersection without at least one joint angle reaching either zero or π .*

Proof: Adjacent links cannot intersect without the internal angle between them reaching 0. Pick a link; call it the base. (See figure 13.) Call the endpoints of the opposite link a and b . Intersection between the links must first occur when a or b is coplanar with the base. If a is coplanar with the base, then the joint angle between the base and the adjacent link containing a must be one of 0 or π ; if b , then the joint angle between the base and the adjacent link containing b must be one of 0 or π . ■

If we assume that the origami design is such that it can be folded flat, a stronger result holds:

Theorem 1 *Rigid flat-foldable degree-four origami can only self-intersect when flat.*

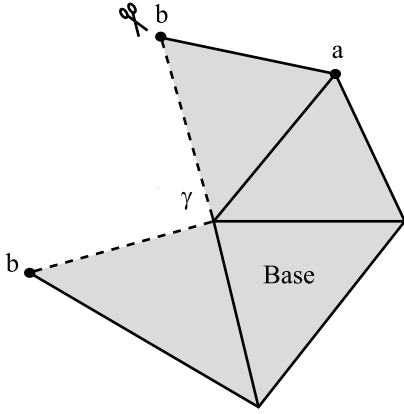


Figure 13: A ‘cut’ degree-four origami mechanism.

Proof: Assume that there is a collision. From lemma 1, at least one crease angle is 0 or π . Label the mechanism so that crease angle is m , and label the sector angles A, B, C , and D as shown in figure 12.

For flat-foldable origami, Kawasaki’s theorem constrains $A + C = \pi$ and $B + D = \pi$; thus for flat-foldable origami, there exists an integer i s.t. $n = m + i\pi$. Since m is 0 or π at a collision, n is an integer multiple of π .

Since at least creases m and n are folded flat, facets A and B are coplanar, as are C and D. Let (AB) be the compound facet containing A and B, and (CD) be the compound facet containing C and D. If these compound facets are coplanar, we are done. If they are not, the structure is that of a simple pair of hinged planes that is collision-free unless flat. (In fact, this is a ‘simple’ fold.) ■

4.2 Single-vertex origami

More advanced origami skills require the simultaneous manipulation of more than four creases. In the remainder of the section, we present the relationship between crease angles for vertices of arbitrary degree; our result is also applicable to the case where there is missing or excess sector angle around the vertex.

The mobility of a vertex of degree n is $n - 3$. We will therefore choose $n - 3$ arbitrary independent crease angles as input, and solve for the remaining crease angles. (In the special case where the dependent crease angles are sequential, a simpler solution is

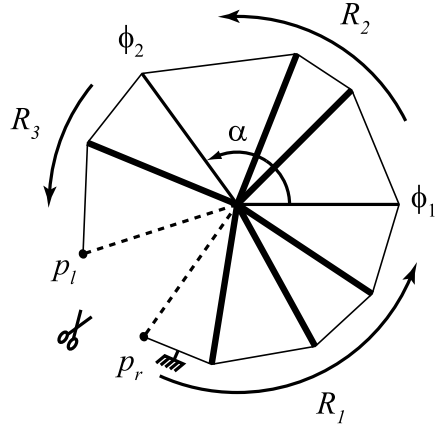


Figure 14: Solving for three dependent crease angles.

possible using the inverse kinematics approach described in [Han and Amato, 2000].)

Figure 14 shows the procedure; φ_1, φ_2 , and φ_3 are the crease angles to be solved for. First cut the crease corresponding to φ_3 , and flatten the paper. For any valid configuration of the paper, the two cut edges must ‘line up’ in such a way that they could be re-glued together. Let p_l and p_r be points along these edges a unit distance from the vertex.

Anchor the facet clockwise from the φ_3 crease, and choose a coordinate system with origin at the vertex and with the x -axis along the φ_1 crease. The point p_r lies at a fixed position within the $z = 0$ plane in this coordinate system.

If p_l were permitted to move, then its location would be given by a sequence of rotations about each of the creases. Let R_x and R_z be matrices describing rotation about the x - and z axes respectively. Let R_1, R_2 , and R_3 be matrices corresponding to rotations about the independent crease angles, as shown in figure 14.

The closure constraint can now be written as

$$R_1 R_x(\varphi_1) R_2 R_z(\alpha) R_x(\varphi_2) R_z(-\alpha) R_3 p_l = p_r, \quad (2)$$

Our goal is to solve for φ_1 and φ_2 , given R_1, R_2 , and R_3 , which may be easily computed from the independent crease angles and the geometry of the paper. Rewrite equation 2:

$$R_x(\varphi_1) Z R_x(\varphi_2) a = b, \quad (3)$$

where Z , a , and b may be computed:

$$Z = R_2 R_z(\alpha) \quad (4)$$

$$a = R_z(-\alpha) R_3 p_l \quad (5)$$

$$b = R_1^T p_r. \quad (6)$$

Multiplying out equation 3 gives three equations, the first of which is

$$k_3 = k_1 \cos \varphi_2 + k_2 \sin \varphi_2, \quad (7)$$

with k_1 , k_2 , and k_3 computed to be

$$k_1 = z_{12} a_2 + z_{13} a_3 \quad (8)$$

$$k_2 = z_{13} a_2 - z_{12} a_3 \quad (9)$$

$$k_3 = b_1 - z_{11} a_1. \quad (10)$$

If $k_1 = k_2 = 0$, then equation 7 implies that φ_2 can take on any value. Otherwise, equation 7 has the solution(s)

$$\varphi_2 = \text{atan}(k_2, k_1) \pm \text{acos} \left(\frac{k_3}{\sqrt{k_1^2 + k_2^2}} \right). \quad (11)$$

There may be zero, one, two, or infinitely many solutions for φ_2 . For each value of φ_2 , the remaining two rows of equation 3 can be used to solve for φ_1 , which either has a unique value or is unconstrained. φ_3 is uniquely determined by the angle between the normals to the facets at either end of the cut chain.

4.3 Multi-vertex origami

For a single vertex of degree n , we can view $n - 3$ of the creases as ‘inputs’, and 3 of the creases as ‘outputs’. Given the dihedral angles at the input creases, equation 11 and the results of the previous section can be used to compute the dihedral angles at the output creases.

Some folds require that multiple connected vertices be manipulated simultaneously. Figure 15 shows a network of four vertices.

An output from one vertex can be viewed as the input to the adjacent vertex. Therefore, any labeling of the creases as either output or input that satisfies the property that each vertex has three outputs can therefore be used to construct a local parameterization of the configuration space, and simulate local motion of the crease network.

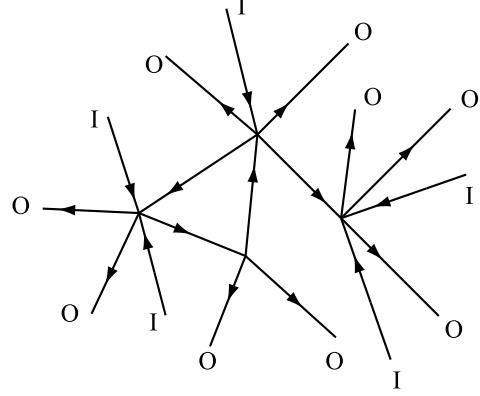


Figure 15: A multi-vertex pattern with a mobility of five.

5 The topology of origami configuration space

The parameterizations described in section 4.2 allow simulation and local planning for origami and other spherical n -bar linkages. However, they have some disadvantages:

1. The configuration of a rigid origami mechanism is completely determined by the dihedral angles, but not all choices of dihedral angles satisfy the constraints imposed by the geometry of the paper and the crease pattern.
2. The parameterizations are not global: the mapping from certain input joint angles to output joint angles may be one-to-many.
3. Finding a trajectory from start to goal that satisfies the constraints can be difficult. The space of configurations may have multiple components, or sections of the configuration space may be joined only at specific regions along their boundaries. Parameterizations give no information about the connectedness of configuration space.

This section describes the connectedness and topology of configuration spaces of n -bar spherical closed chains. The analysis uses techniques described in Milgram and Trinkle [Milgram and Trinkle, ming].

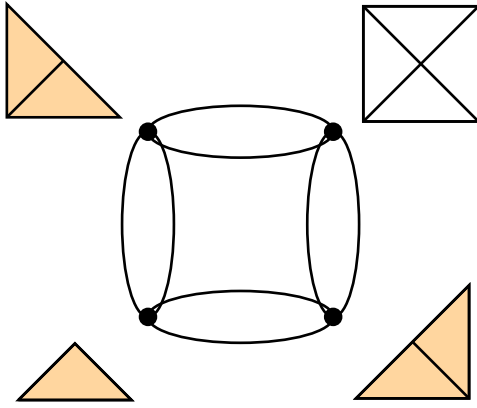


Figure 16: Four flat configurations of a square piece of paper with two diagonal creases, and the topological structure of the associated configuration space.

5.1 Four- and five-bar mechanisms

Figure 17 shows an example, for the case where the first two sector angles counterclockwise from the horizontal are equal. We first cut the paper along one of the creases, as shown. If the crease angles were known for creases 1 and 2, then the configuration of the mechanism would be completely determined. However, there is an additional constraint – that the crease angles of the uncut creases be such that the edges of the cut crease ‘line up’. We will therefore analyze the behavior of a point on the cut crease (points A and B in the figure), and see how it restricts motion of the other creases.

We label the creases as shown in figure 17, cut crease 3, and rigidly attach the facet between creases 1 and 4 to the ground. Consider the motion of the point A as the paper is allowed to fold along creases 1 and 2. Point A is a fixed distance from the central vertex, and can move on the surface of a sphere. Its motion is also bounded on the left by a plane normal to crease 1, and containing point A. There are two configurations of crease angles 1 and 2 that allow point A to reach most locations on the sphere: crease 2 may be convex, or concave. There are some locations that can only be reached in one way: those that fall on the plane normal to crease 1 and containing point A. There is also one point that can be reached in an infinite number of ways, at the intersection of crease 1 and the sphere.

Now consider point B, that rotates around crease 4. The reachable locations form a circle that lies in a plane perpendicular to crease 4.

If the cut is removed, point A and point B must touch; we will call this point AB. AB must move on the intersection of the sphere cut by a plane that A moves on, and the circle that B moves on. The locations that AB can reach therefore form an arc of a circle.

We can describe the space of possible configurations of the paper by the ways in which point AB can reach each point on the arc. There are two configurations that reach each point on the interior of the arc (crease 2 may be either concave or convex). There is only one way in which each of the endpoints of the arc can be reached – crease 2 is flat at each endpoint.

Each point on the arc corresponds to a slice of the space of configurations of the paper, described by crease angles 1 and 2. Starting at one endpoint of the arc, the slice is a single configuration. Moving continuously along the arc, each new slice corresponds to two configurations. At the final slice (at the other endpoint of the arc), there is only one configuration. The topology of this shape, and thus of the configuration space, is a circle – a 1-dimensional manifold with one component.

In general, the set of reachable locations of point A is a sphere bounded by two planes perpendicular to crease 1. The intersection of this surface with the circle reachable by point B can be a circle, an arc of a circle, or two arcs of a circle. Depending on the shape of this workspace, and the ways in which point AB can reach each point on the workspace, the configuration space may have one of several different structures, as shown in figure 18.

- *Null intersection.* One side of the circle may be completely contained in the workspace. The pre-image of an arc completely contained within the workspace is two arcs.
- *Transverse intersection.* One side of the circle may be cut by the bounding plane at two points. The pre-image of an arc touching the bounding plane is an arc.
- *Tangent intersection.* The circle just touches a bounding circle of non-zero radius. The pre-image of an arc tangent to the bounding circle is a pair of arcs touching at a single interior point.

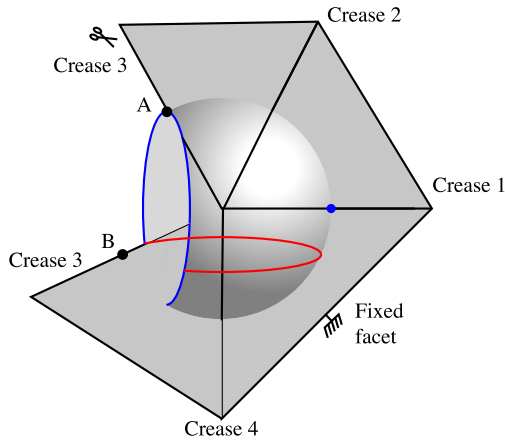


Figure 17: A degree-four vertex, cut along crease 3.

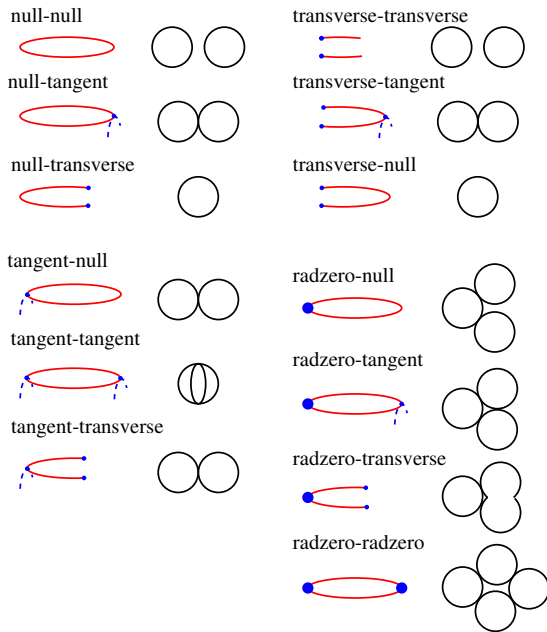


Figure 18: Thirteen of the sixteen possible ways a circle can intersect the workspace of an open three-bar spherical chain. For each class, the ellipses on the left show the workspace; the circles on the right show the configuration space (the pre-image of the workspace). There are seven distinct topological classes of configuration space.

- *Radius-zero intersection.* The circle touches the bounding plane at one of the poles of the sphere on the x axis. The pre-image of this point is a circle of configurations corresponding to spinning links about the x axis; the pre-image of an arc through this point is two arcs connected by a circle.
- We ignore the case where the circle is completely contained within the boundary of the open workspace.

Five-bar mechanisms may be analyzed by fixing one of the dihedral angles, analyzing the resulting four-bar mechanism, and considering how the topology of the four-bar configuration space changes as the (initially) fixed dihedral angle is varied.

5.2 Many-link mechanisms

As can be seen from the analysis of four-bar mechanisms in the previous section, the structure of the configuration space origami can be very complicated, even if we ignore self-intersections. In order to design a motion planner, or to write an algorithm that determines if paths between two configurations exist, we would like to know whether the configuration space is a manifold, where it branches into separate sections, and if there are lower-dimensional regions that connect different sections of the space.

The idea behind the graphical analysis of the topology of configuration spaces is to cut the mechanism and analyze an open chain with $n - 2$ revolute joints to determine the ways that the open chain can reach each point in the workspace. We then consider the curve of points, that the endpoint of the remaining chain, with one revolute joint, can reach. The pre-image of the forward kinematics map for the $(n - 2)$ -joint arm at each point on that curve corresponds to a slice of the configuration space for the mechanism. The topology of these slices only changes at critical (or singular) configurations of the arm.

In this section, we more formally analyze the configuration space in terms of the singularities and the workspace of an open spherical chain, using tools from Morse theory. In this analysis, we ignore joint limits and self-intersections.

We have not developed a practical planning algorithm for high-degree-of-freedom origami closed chains, but the

theorem and corollaries in this section yield some insight into the structure of the configuration space, W . The theorems and proofs essentially track Milgram and Trinkle's [Milgram and Trinkle, ming] results for planar and spatial closed chains with ball joints, which they have used to design a complete motion planner for those systems.

A possibly more complete, analysis of the configuration space of origami mechanisms is presented by Kapovich and Millson [Kapovich and Millson, 1995]; our method has the advantage of a relatively simple geometric interpretation, and a graphical method for determining whether the configuration space is a manifold.

Theorem 2 describes the singularities, or critical points, of the forward kinematics map for the $(n-2)$ -joint chain, in terms of the crease angles. Corollary 1 describes the image of these critical points on the sphere on which the endpoint of the cut chain can move: a set of circles all perpendicular to the first axis. (The circle containing the point A in figure 17 is an example of such a circle, but in longer chains, there may also be several circles interior to the workspace of A.)

Corollary 2 then considers the relationship between the workspace of the $(n-2)$ -joint chain, and the configuration space of the entire origami mechanism, W . Specifically, we let γ be the curve traced by the single-link mechanism (the circular arc traced by B, in figure 17; the configuration space W is the pre-image of the intersection of γ and the workspace of the $(n-2)$ -joint chain under the forward kinematics map. Specifically, we show that the configuration space is a manifold iff γ intersects each critical circle transversally.

The following definitions are taken from Milnor [Milnor, 1997]. We say that a map between two manifolds is *smooth* if all of the partial derivatives exist and are continuous. Consider a smooth map $f : M \mapsto N$, from a manifold of dimension m to a manifold of dimension n . Let C be the set of all $x \in M$ such that

$$df_x : TM_x \mapsto TN_{f(x)}$$

has rank less than n (is not onto). Then C will be called the set of *critical points*, $f(C)$ the set of *critical values*, and the complement $N - f(C)$ the set of *regular values* of f .

Consider the *forwards kinematics map* $f : M \mapsto N$ from the torus $M = S^1 \times S^1 \times \dots \times S^1$ of dihedral angles

to the workspace of an endpoint on the last facet. The map can be written as a product of rotation matrices applied to the initial location of the endpoint, and is smooth.

The workspace N may be constructed iteratively. Spin the endpoint around the $m-1$ axis, creating a circle with radius dependent on sector angle β_{m-1} . Call this circle N_{m-1} . Spin the circle around the $m-2$ axis; call the result N_{m-2} . Since all axes intersect at the origin, N_{m-2} is a section of a sphere, bounded by two half-planes perpendicular to the $m-2$ axis. Spin each resulting workspace around the preceding axis. The workspace N is equal to N_1 , and is the intersection of the unit sphere S^2 with two halfspaces with normals pointing along the first axis. N is therefore either a two-manifold or a two-manifold with boundary.

Theorem 2 *Consider an open spherical chain with all sector angles $B_0 \dots B_{n-1}$ less than π . The critical points of the forwards kinematics map which sends a configuration of the chain to its endpoint are the configurations for which the first dihedral angle ranges over $[0, 2\pi)$, and each of the remaining dihedral angles is one of $\{0, \pi\}$.*

Proof: The configurations of the system can be described by a list of vectors corresponding to the current location of the endpoint X_n and each axis X_i in the workspace,

$$q = (X_1, X_2, \dots, X_n), \quad (12)$$

with the constraints

$$\|X_i\| = 1 \quad (13)$$

$$\angle X_i X_{i+1} = \beta_i. \quad (14)$$

The linear map df_θ between the tangent spaces of the torus and the workspace can be described by the Jacobian of f . Use the cross-product method to write the Jacobian:

$$J_f = [X_1 \times X_n \quad | \quad X_2 \times X_n \quad | \quad \dots \quad | \quad X_{n-1} \times X_n] \quad (15)$$

If $X_1 \dots X_n$ lie in a plane, then the Jacobian has rank less than two, and the configuration is a critical point. Proof of the converse: X_1 and X_2 are linearly independent, so at least one column of the Jacobian (either $X_1 \times X_n$ or $X_2 \times X_n$) is non-null. All axes and the endpoint must lie in a plane perpendicular to this column. Since $X_1 \dots X_n$ lie in a plane iff all of the dihedral angles except the first are one of $\{0, \pi\}$, this completes the proof. ■

Corollary 1 *The critical values of f are the circles formed by rotating the points $(\cos \rho_k, \sin \rho_k)$ around the X_1 axis, where k ranges over $0 \dots 2^{n-1}$, and*

$$\rho_k = \sum_{i=1}^{n-1} (-1)^{e_{i-1}(k)} \beta_i, \quad (16)$$

with $e_i(k)$ denoting the i th bit of k .

Lemma 1 from Milnor [Milnor, 1997] states that if $f : M \mapsto N$ is a smooth map between manifolds of dimension $m \geq n$, and if $y \in N$ is a regular value, then the set $f^{-1}(y) \subset M$ is a smooth manifold of dimension $m - n$.

Corollary 2 *Let γ be a curve on the unit sphere that intersects critical circles only at discrete points, and that does not contain any critical circles of radius 0, and let $W = f^{-1}(\gamma)$. W is a differentiable manifold if and only if γ intersects each critical circle transversally.*

Proof: Assume the curve γ is described by a pair of constraints of the form

$$p(x, y, z) = 0 \quad (17)$$

$$x^2 + y^2 + z^2 = 1, \quad (18)$$

where p has the property that its gradient ∇p is normal to the unit sphere.

The algebraic variety W is a subset of the torus of dihedral angles, and can be described by the composition of the constraints described by equation 17 with the forwards kinematic map f . Since the forwards kinematic map already constrains the endpoint to lie on the unit sphere, along any path $\theta(t)$ contained in the variety W ,

$$\frac{d}{dt} p(f(\theta(t))) = \nabla p^T \dot{f} = \nabla p^T J_f \dot{\theta} = 0. \quad (19)$$

So the Jacobian of the variety W is

$$J_C = \nabla p^T J_f \quad (20)$$

$$= \left[\nabla p^T (X_1 \times X_n) \quad \dots \quad \nabla p^T (X_{n-1} \times X_n) \right]. \quad (21)$$

The Jacobian has only one row, and describes the normal to W . At any regular point of f , at least two of the

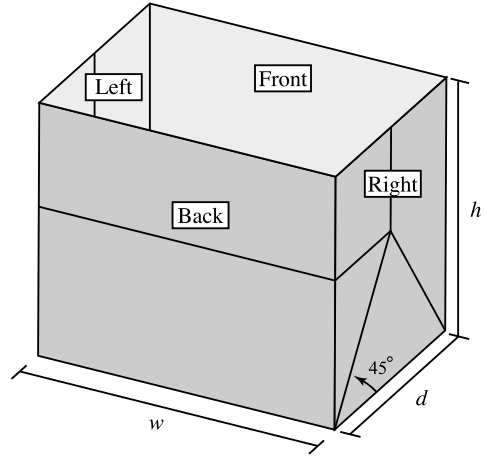


Figure 19: A shopping bag with the traditional crease pattern.

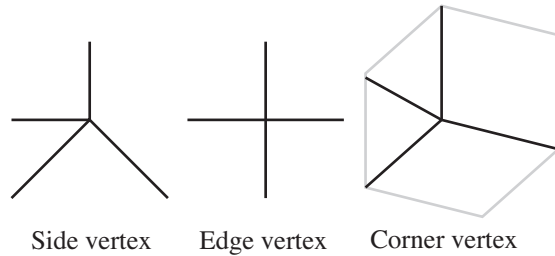


Figure 20: The three types of vertex found in a shopping bag.

cross products will be linearly independent, and the rank of J_W is therefore one. At a critical point of f where γ is transverse to the critical circle, ∇p makes a non-zero dot product with $X_1 \times X_n$, and the rank of J_W is one. At a critical point of f where γ is tangent to the critical circle, every dot product is zero, and J_W is degenerate. ■

6 An example of 3D (non)-foldability: the paper shopping bag

The Bellows Theorem, proven in 1997 [Connolly et al., 1997] states that “any continuous flex that preserves the edge-lengths of a closed triangu-

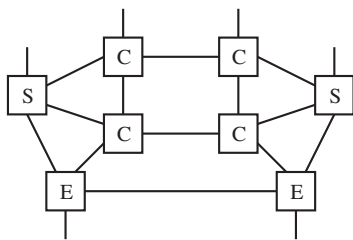


Figure 21: The vertex graph for a shopping bag. The nodes represent ‘edge’, ‘side’, and ‘corner’ vertices, and the edges represent creases that connect vertices.

lated surface of any genus in three-space must flex in such a way that the volume it bounds stays constant.”

This implies that no polyhedron with a fixed, finite number of creases is sufficient to model the deflation of a closed airbag, or the inflation of a teabag or origami waterbomb. But where are the boundaries? What origami structures can or cannot be satisfactorily modeled with fixed crease patterns?

In this section, we consider what is probably the most commonplace origami-like structure: the paper shopping bag. Perhaps surprisingly, it turns out that a shopping bag with rigid facets, and creases in the usual places, cannot be folded flat. Specifically, the bag has a configuration space that is just isolated points corresponding to the flat and fully open states. This might be considered a design feature; since the facets resist bending and crinkling, the bag tends to stay in its current configuration, either open or closed.

Figure 19 shows the traditional crease pattern for a shopping bag. The height of the bag is h , the width is w , and the depth is d . We assume that $h > d/2$; this ensures that the diagonal creases on the right and left sides of the bag meet.

We can distinguish three types of vertex; see figure 20. The vertices in the middle of each of the right and left sides of the bag have sector angles of $(90^\circ, 135^\circ, 90^\circ, 45^\circ)$. There is a vertex along each of the two of the upright edges of the bag, with sector angles $(90^\circ, 90^\circ, 90^\circ, 90^\circ)$. There are vertices at the corners of the bag with sector angles $(90^\circ, 90^\circ, 45^\circ, 45^\circ)$.

Some pairs of vertices share a crease; figure 21 shows how vertices of each type are connected to one another.

We can use equation 1 to show that the shopping bag

cannot be folded by bending facets.

Fact 3 *A piecewise rigid shopping bag with the traditional crease pattern cannot be continuously folded between the open and closed states.*

Proof: Consider an ‘edge’ vertex. There are four $\pi/2$ sector angles, so equation 1 implies that the two vertical creases that meet at this vertex have crease angles that are equal in magnitude. Assume that the magnitude of these crease angles is 0 or π . In this case, it is easy to show by traversing the vertex graph and applying 1 that the bag is flat, and we are done.

If the magnitude is not 0 or π , then the two horizontal creases from this vertex must be one of $\{0, \pi\}$. Choose a crease that is 0 or π , and connected to another vertex. Walk the crease network; each of the left and right sides is flat (open or folded), and each of the corners is either fully open or collapsed. ■

The following observations can be made:

1. A shopping bag with creases in the ‘usual’ places is rigid.
2. Two shopping bags taped together at their tops cannot be flattened with a finite number of fixed creases. (Thanks to Robert Lang for this example of the bellows theorem.)
3. A shopping bag cannot be turned inside-out with a finite number of fixed creases. (According to Erik Demaine, it has been proven by Connelly that a convex vertex cannot be turned inside out using a finite number of creases, but this work may not yet have been published.) Robert Lang points out that this work implies that the ‘closed sink’ origami move that inverts a convex vertex cannot be modeled with a finite number of creases.

A natural question is whether a shopping bag can be folded by adding a finite number of creases. With Erik and Martin Demaine, we have shown that it can, and a future paper will discuss this and other problems of 3D foldability.

7 Conclusion

The paper has presented the first origami-folding robot, and an initial exploration into issues regarding folding manipulation.

There are several promising directions for future work, including far more capable machines for folding, and mathematical tools for analyzing more general models of foldability.

We are particularly interested in ‘low-level’ manipulation skills (like landmarking) that humans use to precisely and reliably place creases in flexible paper. We also intend to explore further aspects of complex closed-chain manipulation. The configuration spaces of closed chains can be complicated, and understanding connectedness of these c-spaces is still an open problem.

Another interesting problem is understanding multi-vertex patterns like that shown in figure 15. Although we have presented a simple parameterization of the configuration space for multi-vertex patterns, topological analysis to determine the connectedness of such spaces seems to be a challenging problem.

Acknowledgments

Thanks to Erik and Martin Demaine, Robert Lang, Zhong You, Jeffrey Trinkle, Douglas James, and James Kuffner for their many discussions and contributions to the present work. The graphical method described in section 5.1 is based on discussions with James Milgram.

The work of Devin Balkcom was supported by a Department of Energy Computational Science graduate fellowship. Funding was further provided by NSF grants IIS 0082339 and IIS 0222875.

References

- [Ascher and Lin, 1999] Ascher, U. and Lin, P. (1999). Sequential regularization methods for simulating mechanical systems with many closed loops. *SIAM Journal on Scientific Computing*, 21(4):1244–1262.
- [Aumann, 1991] Aumann, G. (1991). Interpolation with developable Bézier patches. *Computer Aided Geometric Design*, 8:409–420.
- [Balkcom, 2004] Balkcom, D. J. (2004). Robotic origami folding. Ph.D. Thesis, published as Carnegie Mellon University RI TR 04-43.
- [Balkcom and Mason, 2004] Balkcom, D. J. and Mason, M. T. (2004). Introducing robotic origami folding. In *IEEE International Conference on Robotics and Automation*, pages 3245–3250.
- [Baraff and Witkin, 1998] Baraff, D. and Witkin, A. (1998). Large steps in cloth simulation. In *SIGGRAPH*, pages 43–54.
- [Bridson et al., 2002] Bridson, R., Fedkiw, R., and Anderson, J. (2002). Robust treatment of collisions, contact, and friction for cloth animation. In *SIGGRAPH*.
- [Choi and Ko, 2002] Choi, K.-J. and Ko, H.-S. (2002). Stable but responsive cloth. In *SIGGRAPH*.
- [Connelly et al., 1997] Connelly, R., Sabitov, I., and Walz, A. (1997). The bellows conjecture. *Contributions to Algebra and Geometry*, 38(1):1–10.
- [Dai and Jones, 1999] Dai, J. and Jones, J. R. (1999). Mobility in metamorphic mechanisms of foldable/erectable kinds. *Transactions of ASME: Journal of Mechanical Design*, 121(3):375–382.
- [Dai and Jones, 2002a] Dai, J. and Jones, J. R. (2002a). Carton manipulation analysis using configuration transformation. *Journal of Mechanical Engineering Science*, 216(5):543–555.
- [Dai and Jones, 2002b] Dai, J. and Jones, J. R. (2002b). Kinematics and mobility analysis of carton folds in packing manipulation based on the mechanism equivalent. *Journal of Mechanical Engineering Science*, 216(10):959–970.
- [Dai and Jones, 2005] Dai, J. and Jones, J. R. (2005). Matrix representation of topological configuration transformation of metamorphic mechanisms. *Transactions of the ASME: Journal of Mechanical Design*, 127(4):837–840.
- [Demaine and Demaine, 2001] Demaine, E. D. and Demaine, M. L. (2001). Recent results in computational origami. In *Proceedings of the 3rd International Meeting of Origami Science, Math, and Education*.

- [Gupta et al., 1998] Gupta, S., Bourne, D., Kim, K. K., and Krishnan, S. S. (1998). Automated process planning for robotic sheet metal bending operations. *Journal of Manufacturing Systems*.
- [Han and Amato, 2000] Han, L. and Amato, N. M. (2000). A kinematics-based probabilistic roadmap method for closed chain systems. In *Workshop on the Algorithmic Foundations of Robotics*, pages 233–246.
- [Hilbert and Cohn-vossen, 1952] Hilbert, D. and Cohn-vossen, S. (1952). *Geometry and the Imagination*. Chelsea.
- [Huffman, 1976] Huffman, D. (1976). Curvature and creases: A primer on paper. *IEEE Transactions on Computers*, C-25(10):1010–1019.
- [Hull, 1994] Hull, T. C. (1994). On the mathematics of flat origamis. In *Congressus Numerantium*, volume 100, pages 215–224.
- [Kapovich and Millson, 1995] Kapovich, M. and Millson, J. (1995). On the moduli space of polygons in the Euclidean plane. *Journal of Differential Geometry*, 42(1):133–164.
- [Kergosien et al., 1994] Kergosien, Y. L., Gotoda, H., and Kunii, T. L. (1994). Bending and creasing virtual paper. In *IEEE Computer Graphics and Applications*, pages 40–48.
- [Lang, 2001] Lang, R. (2001). Trees and circles: an efficient algorithm for origami design. In *Proceedings of the 3rd International Meeting of Origami Science, Math, and Education*.
- [Leopoldseder and Pottmann, 1998] Leopoldseder, S. and Pottmann, H. (1998). Approximation of developable surfaces with cone spline surfaces. *Computer Aided Design*, 30:571–582.
- [Liu and Dai, 2003] Liu, J. and Dai, J. (2003). An approach to carton-folding trajectory planning using dual robotic fingers. *Robotics and Autonomous Systems*, 42:47–63.
- [Lu and Akella, 1999] Lu, L. and Akella, S. (1999). Folding cartons with fixtures: A motion planning approach. In *IEEE International Conference on Robotics and Automation*.
- [Lu and Akella, 2000] Lu, L. and Akella, S. (2000). Folding cartons with fixtures: A motion planning approach. *IEEE Transactions on Robotics and Automation*, 16(4):346–356.
- [Milgram and Trinkle, ming] Milgram, R. J. and Trinkle, J. (forthcoming). The geometry of configurations spaces for closed chains in two and three dimensions. *Homology, Homotopy, and Applications*.
- [Milnor, 1997] Milnor, J. (1997). *Topology from the Differentiable Viewpoint*. Princeton Landmarks in Mathematics. Princeton University Press.
- [Miyazaki et al., 1992] Miyazaki, S., Yasuda, T., Yokoi, S., and Toriwaki, J. (1992). An interactive simulation system of origami based on virtual space manipulation. In *Proceedings of the IEEE International Workshop on Robot and Human Communication*, pages 210–215.
- [Pottmann and Wallner, 1999] Pottmann, H. and Wallner, J. (1999). Approximation algorithms for developable surfaces. *Computer Aided Geometric Design*, 16:539–556.
- [Redont, 1989] Redont, P. (1989). Representation and deformation of developable surfaces. *Computer Aided Design*, 21(1):13–20.
- [Rodrigues-Leal and Dai, 2007] Rodrigues-Leal, E. and Dai, J. (2007). From origami to a new class of centralized 3-DOF parallel mechanisms. In *Proceedings of the 31st ASME Mechanisms and Robotics Conference*.
- [Sun and Fiume, 1996] Sun, M. and Fiume, E. (1996). A technique for constructing developable surfaces. In *Graphics Interface*, pages 176–185.
- [Weiss and Furtner, 1988] Weiss, G. and Furtner, P. (1988). Computer-aided treatment of developable surfaces. *Computers and Graphics*, 12(1):39–51.